

# Theoretical Study of Tungsten $\eta^3$ -Silaallyl/ $\eta^3$ -Vinylsilyl and Vinyl Silylene Complexes: Interesting Bonding Nature and Relative Stability

Mausumi Ray,<sup>†</sup> Yoshihide Nakao,<sup>†</sup> Hirofumi Sato,<sup>†</sup> and Shigeyoshi Sakaki\*,<sup>‡,§</sup>

Department of Molecular Engineering, Graduate School of Engineering, Kyoto University, Kyotodaiigaku-Katsura, Nishikyo-ku, Kyoto 615-8510, and Fukui Institute for Fundamental Chemistry, Nishihiraki-cho Takano, Kyoto 606-8103, Japan

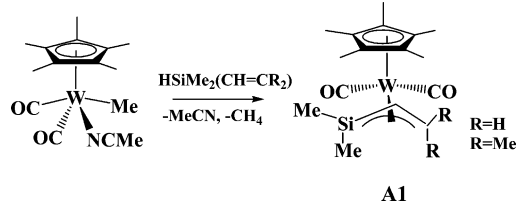
Received June 14, 2007

The geometries and bonding nature of interesting new tungsten  $\eta^3$ -silaallyl/ $\eta^3$ -vinylsilyl complex  $\text{Cp}^*(\text{CO})_2\text{W}(\eta^3\text{-H}_2\text{SiCHCH}_2)$  (**1**) and tungsten vinyl silylene complex  $\text{Cp}(\text{CO})_2\text{W}(\text{CHCH}_2)(\text{SiH}_2)$  (**2**) and the conversion reaction of **1** to **2** were theoretically investigated with the density functional theory (DFT) and CCSD(T) methods, where **1** was adopted as a model of  $\text{Cp}^*(\text{CO})_2\text{W}(\eta^3\text{-Me}_2\text{SiCHCMe}_2)$ . The nonbonding  $\pi$  orbital ( $\varphi_{n\pi}$ ) of the  $\eta^3\text{-H}_2\text{SiCHCH}_2$  group is similar to that of the  $\eta^3$ -allyl group except that the Si p orbital more contributes to  $\varphi_{n\pi}$  than the C p orbital. On the other hand, the  $\pi$  orbital ( $\varphi_\pi$ ) of the  $\eta^3\text{-H}_2\text{SiCHCH}_2$  group is considerably different from that of the  $\eta^3$ -allyl group; the  $\pi$ -conjugation between the Si and C atoms is very weak, unlike that of the  $\eta^3$ -allyl group in which  $\pi$ -conjugation is considerably strong. Thus, **1** can be understood to be a species between tungsten  $\eta^3$ -vinylsilyl and tungsten  $\eta^3$ -silaallyl complexes. From the geometry and frontier orbitals, **2** can be understood to be a tungsten vinyl silylene complex in which charge transfer interaction between the silylene and vinyl groups is very weak. Complex **1** is much more stable than **2** by 21.0 (20.9) kcal/mol, but  $\text{Cp}(\text{CO})_2\text{W}(\eta^3\text{-H}_2\text{SiCCH})$  (**3**) is less stable than  $\text{Cp}(\text{CO})_2\text{W}(\text{CCH})(\text{SiH}_2)$  (**4**) by 0.7 (4.9) kcal/mol, where the CCSD(T)- and DFT-calculated values are given without and in parentheses, respectively. This means that the tungsten  $\eta^3$ -silaallyl/ $\eta^3$ -vinylsilyl complex can be isolated but the tungsten vinyl silylene complex cannot, unlike the tungsten acetylidyne silylene complex  $\text{Cp}^*(\text{CO})_2\text{W}(\text{CC}'\text{Bu})(\text{SiPh}_2)$  which was isolated recently. Complex **1** converts to **2** with a large activation barrier of 34.2 (33.2) kcal/mol, while **3** easily converts to **4** with a moderate activation barrier of 15.8 (15.3) kcal/mol. These differences between **1** and **3** can be interpreted as follows: Though the Si–C bond is weak in **1**, the W–( $\eta^3\text{-H}_2\text{SiCHCH}_2$ ) interaction is considerably strong. Moreover, the W–vinyl and silylene–vinyl interactions are very weak in **2**. On the other hand, the Si–C bond is strong but the W–( $\eta^3\text{-H}_2\text{SiCCH}$ ) interaction is weak in **3**. Moreover, the W–acetylidyne and silylene–acetylidyne interactions are very strong in **4**. The reasons are discussed in detail.

## Introduction

The silaallyl species is of considerable interest because it is the simplest of all conjugate systems including the Si element. Unfortunately, the silaallyl species is not stable and a free silaallyl species has not been isolated yet, to our knowledge.<sup>1–3</sup> However, interaction with a transition-metal complex is expected to stabilize the silaallyl species. In this regard, transition-metal complexes of  $\eta^3$ -1-silaallyl ( $\eta^3\text{-H}_2\text{SiCHCH}_2$ ) are interesting compounds in coordination chemistry, organometallic chemistry, and synthetic chemistry.<sup>1–4</sup> Many efforts were made to isolate a transition-metal  $\eta^3$ -silaallyl complex, as follows: In 1976, Sakurai and his collaborators reported the preparation of  $\eta^3$ -1-

Scheme 1. Formation of  $\text{Cp}^*(\text{CO})_2\text{W}(\eta^3\text{-Me}_2\text{SiCHCR}_2)$  (**A1**)



silapropenyl complexes of iron(II).<sup>1a</sup> However, the same authors corrected that the compound synthesized was actually the  $\eta^2$ -vinylsilane complex of iron.<sup>1b</sup> The  $\eta^3$ -1-silaallyl complex  $\text{Cp}^*(\text{PMe}_3)\text{Ru}(\eta^3\text{-Ph}_2\text{SiCHCH}_2)$  was synthesized by thermolysis of  $\text{Cp}^*(\text{PMe}_3)_2\text{Ru}\{\text{Si}(\text{CH}=\text{CH}_2)\text{Ph}_2\}$ , but details were not presented.<sup>4</sup> Recently, a stable tungsten  $\eta^3$ -1-silaallyl complex,  $\text{Cp}^*(\text{CO})_2\text{W}(\eta^3\text{-Me}_2\text{SiCHCMe}_2)$  (**A1**), was successfully isolated via Si–H  $\sigma$ -bond activation of dimethylvinylsilane  $\text{HMe}_2\text{Si}(\text{CH}=\text{CMe}_2)$  with  $\text{Cp}^*(\text{CO})_2\text{W}(\text{MeCN})\text{Me}$ , as shown in Scheme 1.<sup>5</sup> The  $\eta^3$ -coordination of  $\text{Me}_2\text{SiCHCMe}_2$  was clearly seen in its X-ray structure. In the reaction of  $\text{Cp}^*(\text{CO})_2\text{W}(\text{MeCN})\text{Me}$  with similar diphenylalkynylsilane  $\text{HPh}_2\text{Si}(\text{C}\equiv\text{C}'\text{Bu})$ , on the other

\* To whom correspondence should be addressed. E-mail: sakaki@molen.kyoto-u.ac.jp.

<sup>†</sup> Kyoto University.

<sup>‡</sup> Fukui Institute for Fundamental Chemistry.

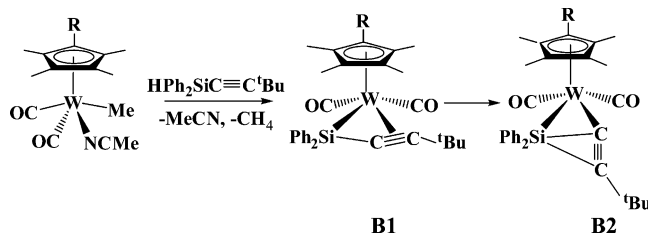
(1) (a) Sakurai, H.; Kamiyama, Y.; Nakadaira, Y. *J. Am. Chem. Soc.* **1976**, *98*, 7453. (b) Sakurai, H.; Kamiyama, Y.; Mikoda, A.; Kobayashi, T.; Sasaki, K.; Nakadaira, Y. *J. Organomet. Chem.* **1980**, *201*, C14. (c) Sakurai, H.; Kamiyama, Y.; Nakadaira, Y. *J. Organomet. Chem.* **1980**, *184*, 13.

(2) Radnia, P.; McKennis, J. S. *J. Am. Chem. Soc.* **1980**, *102*, 6349.

(3) Dai, X.; Kano, N.; Kako, M.; Nakadaira, Y. *Chem. Lett.* **1999**, 717.

(4) Dysard, J. M.; Tilley, T. D.; Woo, T. K. *Organometallics* **2001**, *20*, 1195.

(5) Sakaba, H.; Watanabe, S.; Kabuto, C.; Kabuto, K. *J. Am. Chem. Soc.* **2003**, *125*, 2842.

**Scheme 2. Formation of  $\text{Cp}^*(\text{CO})_2\text{W}(\text{CC}'\text{Bu})(\text{SiPh}_2)$  (**B2**)**

hand, not a similar tungsten  $\eta^3$ -1-silaalkynyl complex,  $\text{Cp}^*(\text{CO})_2\text{W}(\eta^3\text{-Ph}_2\text{SiCC}'\text{Bu})$  (**B1**), but a tungsten acetylidy silylene complex,  $\text{Cp}^*(\text{CO})_2\text{W}(\text{CC}'\text{Bu})(\text{Ph}_2\text{Si})$  (**B2**), was isolated, while **B1** was proposed as an intermediate in the formation reaction of **B2**, as shown in Scheme 2.<sup>6</sup> We also theoretically investigated **B1** and **B2** and found that their bonding nature and electronic structures were very interesting.<sup>7</sup> Thus, it is worth investigating the bonding nature of the similar  $\eta^3$ -1-silaallyl complex **A1** in comparison with the  $\eta^3$ -1-silapropargyl and the usual  $\eta^3$ -allyl complexes and to clarify the reasons why **A1** was isolated but **B1** was not and why **B2** was isolated but the similar vinyl silylene complex  $\text{Cp}^*(\text{CO})_2\text{W}(\text{CHCMe}_2)(\text{SiMe}_2)$  (**A2**) was not.

In the present work, we theoretically investigated the geometries and bonding nature of  $\text{Cp}(\text{CO})_2\text{W}(\eta^3\text{-H}_2\text{SiCHCH}_2)$  (**1**) and  $\text{Cp}(\text{CO})_2\text{W}(\text{CHCH}_2)(\text{SiH}_2)$  (**2**) and the conversion reaction of **1** to **2** with the density functional theory (DFT), MP2 to MP4(SDTQ), and CCSD(T) methods, where **1** and **2** were adopted as models of **A1** and **A2**, respectively. Our main purposes here are (1) to clarify characteristic features of the geometry and bonding nature of **1** in comparison with its carbon analogue  $\text{Cp}(\text{CO})_2\text{W}(\eta^3\text{-H}_2\text{CCHCH}_2)$  (**1C**) and  $\eta^3$ -1-silapropargyl analogue  $\text{Cp}(\text{CO})_2\text{W}(\eta^3\text{-H}_2\text{SiCCH})$  (**3**), where **3** was adopted as a model of **B1**, (2) to evaluate the relative stabilities of **1** and **2**, and (3) to clarify the reasons why **1** was isolated but the similar tungsten  $\eta^3$ -silapropargyl complex **3** was not and why the tungsten vinyl silylene complex **2** was not isolated but the similar tungsten acetylidy silylene complex  $\text{Cp}(\text{CO})_2\text{W}(\text{CCH})(\text{SiH}_2)$  (**4**) was isolated, where **4** was investigated as a model of **B2**.

### Computational Details

Geometries were optimized with the DFT, where the B3PW91<sup>8,9</sup> functional was adopted for the exchange-correlation terms. This is because the optimized geometry of the similar complex  $\text{Cp}(\text{CO})_2\text{W}(\text{CCR})(\text{SiR}_2)$  by the B3PW91 functional agrees well with the experimental one<sup>6</sup> but the geometry optimized by the B3LYP functional<sup>8,10</sup> is somewhat different from the experimental one, as we reported recently.<sup>7</sup> We ascertained that each equilibrium geometry did not exhibit any imaginary frequency and each transition state exhibited only one imaginary frequency. Energy was

(6) Sakaba, H.; Yoshida, M.; Kabuto, C.; Kabuto, K. *J. Am. Chem. Soc.* **2005**, *127*, 7276.

(7) Ray, M.; Nakao, Y.; Sato, H.; Sakaba, H.; Sakaki, S. *J. Am. Chem. Soc.* **2006**, *128*, 11927.

(8) (a) Becke, A. D. *Phys Rev. A* **1988**, *38*, 3098. (b) Becke, A. D. *J. Chem. Phys.* **1993**, *98*, 5648.

(9) (a) Perdew, J. P. In *Electronic Structure of Solids '91*; Ziesche, P., Eschrig, H., Eds.; Akademie Verlag: Berlin, 1991; p 11. (b) Perdew, J. P.; Chevary, J. A.; Vosko, S. H.; Jackson, K. A.; Pederson, M. R.; Singh, D. J.; Fiolhais, C. *Phys. Rev. B* **1992**, *46*, 6671. (c) Perdew, J. P.; Chevary, J. A.; Vosko, S. H.; Jackson, K. A.; Pederson, M. R.; Singh, D. J.; Fiolhais, C. *Phys. Rev. B* **1993**, *48*, 4978. (d) Perdew, J. P.; Burke, K.; Wang, Y. *Phys. Rev. B* **1996**, *54*, 16533.

(10) (a) Lee, C.; Yang, W.; Parr, R. G. *Phys. Rev. B* **1988**, *37*, 785. (b) Miehlich, B.; Savin, A.; Stoll, H.; Preuss, H. *Chem. Phys. Lett.* **1989**, *157*, 200.

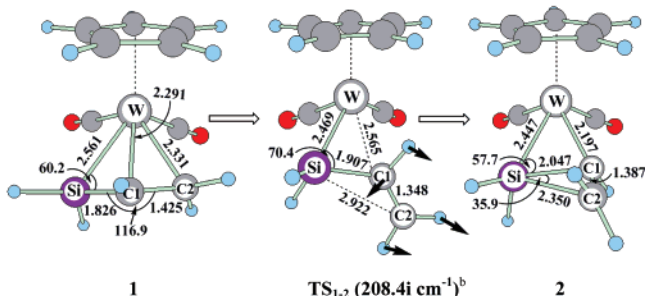


**Figure 1.** Geometry changes by the conversion reaction of  $\text{Cp}(\text{CO})_2\text{W}(\eta^3\text{-H}_2\text{SiCHCH}_2)$  **1** to  $\text{Cp}(\text{CO})_2\text{W}(\text{CHCH}_2)(\text{SiH}_2)$  **2**. The DFT/BS-I method was used. Bond lengths are in angstroms, and bond angles are in degrees. Note indicated by superscript b: The imaginary frequency is given in parentheses. Arrows in  $\text{TS}_{1-2}$  represent important movements of atoms in imaginary frequency.

evaluated with the DFT, MP2 to MP4(SDTQ), and CCSD(T) methods, where the DFT-optimized geometries were adopted.

Two kinds of basis set systems, BS-I and BS-II, were used in this work. In BS-I, the usual LANL2DZ<sup>11</sup> basis set was used for W, cc-pVDZ basis sets<sup>12</sup> were used for Si, C, and O atoms, and the 6-31G basis set was used for H.<sup>13</sup> This BS-I system was employed for geometry optimization. In BS-II, valence electrons of W were represented with the (541/541/111/1) basis set<sup>11,14,15</sup> with the same effective core potentials as those of LANL2DZ. The same basis sets as those of BS-I were used for the other atoms. This BS-II system was employed to evaluate energy changes.

The Gaussian 03 program package<sup>16</sup> was used for all these computations. The Laplacian of the electron density was evaluated with the MOLDEN program package (version 4.6),<sup>17</sup> and molecular orbitals were drawn with the MOLEKEL program package (version 4.3).<sup>18</sup>

### Results and Discussion

In this paper, we report first the geometries and bonding nature of **1** and **2** and then discuss the conversion reaction of **1** to **2** in comparison with the conversion of **3** to **4**. Finally, we discuss the reasons why **1** was isolated but **3** was not.

**Geometry and Bonding Nature of 1.** The optimized geometry of **1** agrees with the experimental one,<sup>5</sup> where the W–Si and W–C2 distances are moderately shorter and the W–C1, Si–C1, and C1–C2 distances are moderately longer than the corresponding experimental values; see Figure 1 and Table 1 for important geometrical parameters. Introduction of Me groups on the C2 and Si atoms leads to excellent agreement of the optimized geometry with the experimental one (see Table 1). The W–Si and W–C2 distances in **1** are moderately longer than those of **3** by 0.033 and 0.022 Å, respectively, and the

(11) Hay, P. J.; Wadt, W. R. *J. Chem. Phys.* **1985**, *82*, 299.

(12) (a) Dunning, T. H., Jr. *J. Chem. Phys.* **1989**, *90*, 1007. (b) Woon, D. E.; Dunning, T. H., Jr. *J. Chem. Phys.* **1993**, *98*, 1358.

(13) (a) Ditchfield, R.; Hehre, W. J.; Pople, J. A. *J. Chem. Phys.* **1971**, *54*, 724. (b) Hehre, W.; Ditchfield, R.; Pople, J. A. *J. Chem. Phys.* **1972**, *56*, 2257.

(14) Couty, M.; Hall, M. B. *J. Comput. Chem.* **1996**, *17*, 1359.

(15) Ehlers, A. W.; Bohme, D. S.; Gobbi, A.; Hollwarth, A.; Jonas, V.; Kohler, K. F.; Stegmann, R.; Veldkamp, A.; Frenking, G. *Chem. Phys. Lett.* **1993**, *208*, 111.

(16) Pople, J. A.; et al. *Gaussian 03*, revision C.02; Gaussian Inc.: Wallingford, CT, 2004. See ref S1 of the Supporting Information for the complete reference for Gaussian 03.

(17) (a) Flükiger, P.; Lüthi, H. P.; Portmann, S.; Weber, J. *MOLEKEL* 4.3; Swiss Center for Scientific Computing: Manno, Switzerland, 2000–2002. (b) Portmann, S.; Lüthi, H. P. *MOLEKEL*, An Interactive Molecular Graphics Tool. *Chimia* **2000**, *54*, 766–770.

(18) Schaftenaar, G.; Noordik, J. H. *MOLDEN*, A Pre- and Post-Processing Program for Molecular and Electronic Structures. *J. Comput.-Aided Mol. Des.* **2000**, *14*, 123–134.

**Table 1. Selected Optimized Parameters<sup>a</sup> of Cp(CO)<sub>2</sub>W( $\eta^3$ -R<sub>2</sub>SiCHCR<sup>1</sup><sub>2</sub>) (R<sup>1</sup> = H or Me; R<sup>2</sup> = H or Me)**

	<b>1</b> (R <sup>1</sup> = H, R <sup>2</sup> = H)	<b>1-Mea</b> (R <sup>1</sup> = Me, R <sup>2</sup> = H)	<b>1-Meb</b> (R <sup>1</sup> = Me, R <sup>2</sup> = Me)	exptl <sup>b</sup> (R <sup>1</sup> = Me, R <sup>2</sup> = Me)
W–Si	2.561	2.549	2.581	2.571
W–C1	2.291	2.303	2.293	2.281
W–C2	2.331	2.454	2.427	2.419
Si–C1	1.826	1.833	1.835	1.801
C1–C2	1.425	1.424	1.427	1.410
–SiC1C2	116.9	120.9	123.9	122.0

<sup>a</sup> The DFT(B3PW91)/BS-I method was used. Bond lengths are in angstroms, and bond angles are in degrees. <sup>b</sup> Reference 5.

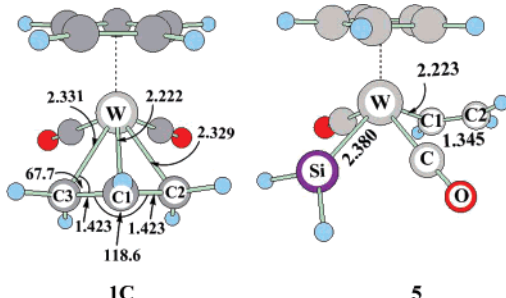
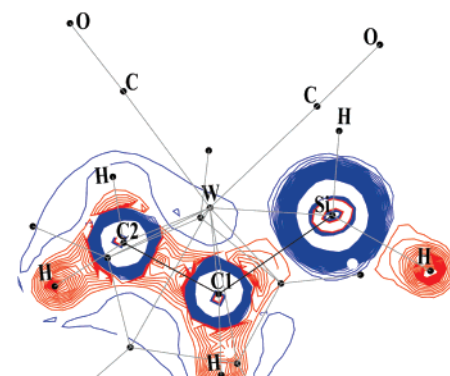


**Figure 2.** Geometries of Cp(CO)<sub>2</sub>W( $\eta^3$ -H<sub>2</sub>CCHCH<sub>2</sub>) **1C** and Cp(CO)<sub>2</sub>W(CHCH<sub>2</sub>)SiH<sub>2</sub> (**5**). The DFT/BS-I method was used. Bond lengths are in angstroms, and bond angles are in degrees.

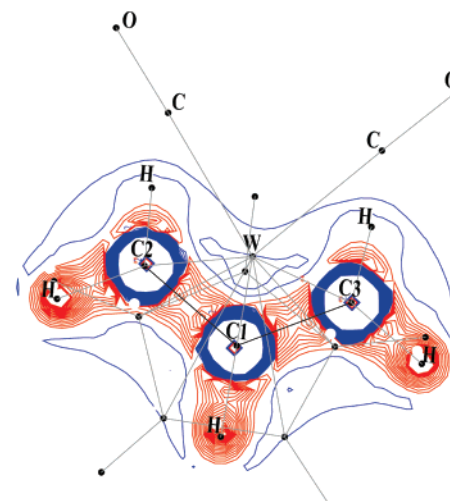
W–C1 distance of **1** is considerably shorter than that of **3** by 0.133 Å (see ref 7 for the optimized geometry of **3**). This significantly shorter W–C1 distance in **1** suggests that the W–C1 interaction is stronger in **1** than in **3**. The SiC1C2 angle of **1** is smaller than that of **3** by 23.1°, because the C1 atom takes sp<sup>2</sup> hybridization in **1** but sp hybridization in **3**.

For better understanding of the geometry and bonding nature of **1**, we optimized tungsten  $\eta^3$ -allyl complex **1C**, as shown in Figure 2. The C1–C2, W–C1, and W–C2 distances and the SiC1C2 angle of **1** are almost the same as those of **1C**.

The Laplacian of the electron density provides clear information on the bonding characteristics.<sup>19–22</sup> The Laplacian plot on the Si–C1–C2 plane of **1** indicates accumulation of electron density between the C1 and C2 atoms but little accumulation of electron density between the Si and C1 atoms, as shown in Figure 3A, where red lines represent accumulation of electron density and blue lines represent depletion of electron density. On the other hand, the Laplacian plot on the C2–C1–C3 plane of **1C** represents accumulation of electron density between the C1 and C2 atoms and between the C1 and C3 atoms (Figure 3B). These results indicate that the Si–C1 interaction in **1** is much weaker than the C3–C1 interaction in **1C** and that the  $\eta^3$ -allyl moiety is well conjugated but  $\eta^3$ -silaallyl is not. In **1**, the Laplacian plots of the W–C1–Si and W–C1–C2 planes exhibit that electron accumulation occurs in the separated regions; one is the region between W and the C1–C2 moiety,



**(A) Cp(CO)<sub>2</sub>W( $\eta^3$ -H<sub>2</sub>SiCHCH<sub>2</sub>) **1****



**(B) Cp(CO)<sub>2</sub>W( $\eta^3$ -H<sub>2</sub>CCHCH<sub>2</sub>) **1C****

**Figure 3.** Laplacian of the electron density on the Si–C1–C2 plane in **1** and on the C3–C1–C2 plane in **1C**. Contour values are 0.0,  $\pm 0.1$ ,  $\pm 0.2$ , .... Red and blue lines represent accumulation of electron density and depletion of electron density, respectively.

and the other is the region between the W and Si atoms, as shown in Figure 4A. In **1C**, on the other hand, electron accumulation occurs in the region between W and the C2–C1–C3 moiety (Figure 4B); note that the electron accumulation between W and the C1–C2 moiety is combined with that between W and the C1–C3 moiety at the C1 atom. From these results, it is concluded that the interaction between W and  $\eta^3$ -H<sub>2</sub>CCHCH<sub>2</sub> is delocalized over three C atoms in **1C** but the interaction between W and  $\eta^3$ -H<sub>2</sub>SiCHCH<sub>2</sub> is not delocalized but separated into two interactions in **1**; one is the interaction between W and the silyl group, and the other is that between W and the vinyl group. In other words, **1** is not a pure tungsten  $\eta^3$ -silaallyl complex, but it is a species between  $\eta^3$ -silaallyl and  $\eta^3$ -silylvinyl complex.

These features presented by the Laplacian plots should be reflected in molecular orbitals. As shown in Figure 5, the HOMO and HOMO – 1 of **1** mainly consist of d orbitals like those of **1C**. The remaining three d orbitals are unoccupied in both **1** and **1C**, which is consistent with the +2 oxidation state of W (d<sup>4</sup> system) in **1** and **1C**. The HOMO – 2 and HOMO – 5 are important in **1** because these two orbitals include the bonding interaction between the H<sub>2</sub>SiCHCH<sub>2</sub> moiety and the

(19) (a) Bader, R. F. W. *Atoms in Molecules: a Quantum Theory*; Clarendon: New York, 1990. (b) Bader, R. F. W. *Chem. Rev.* **1991**, *91*, 893.

(20) Frenking, G.; Fröhlich, N. *Chem. Rev.* **2000**, *100*, 717.

(21) (a) Fan, M. F.; Lin, Z. *Organometallics* **1998**, *17*, 1092. (b) Liu, D.; Lam, K. C.; Lin, Z. *Organometallics* **2003**, *22*, 2827.

(22) (a) Sakaki, S.; Yamaguchi, S.; Musashi, Y.; Sugimoto, M. *J. Organomet. Chem.* **2001**, *635*, 173. (b) Tomita, T.; Takahama, T.; Sugimoto, M.; Sakaki, S. *Organometallics* **2002**, *21*, 4138. (c) Nakajima, S.; Yokogawa, D.; Nakao, Y.; Sato, H.; Sakaki, S. *Organometallics* **2004**, *23*, 4672. (d) Nakajima, S.; Sumimoto, M.; Nakao, Y.; Sato, H.; Sakaki, S.; Osaka, K. *Organometallics* **2005**, *24*, 4029.

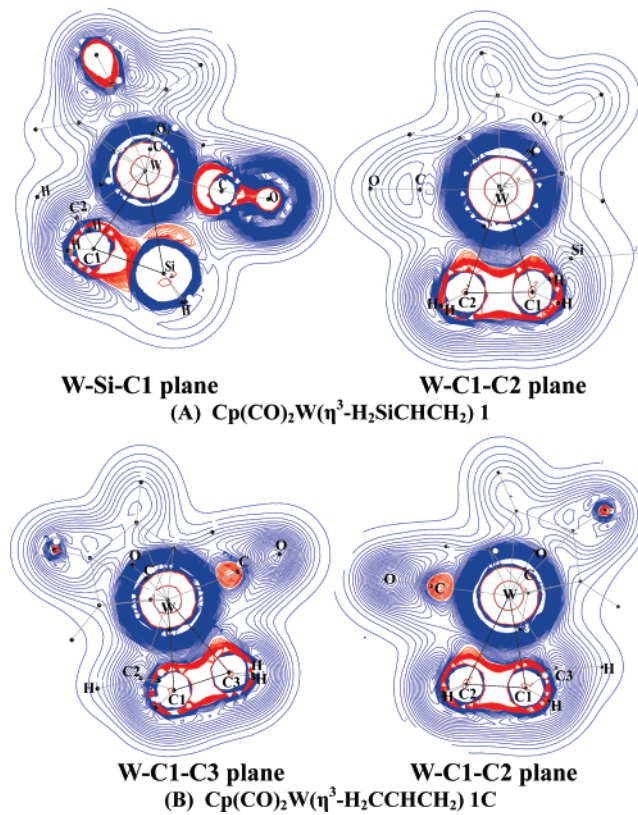


**Figure 4.** Laplacian of the electron density on the W–Si–C1 and W–C1–C2 planes of **1** and on the W–C3–C1 and W–C1–C2 planes of **1C**. Contour values are 0.0,  $\pm 0.01$ ,  $\pm 0.02$ , ... Red and blue lines represent accumulation of electron density and depletion of electron density, respectively.

W center. To discuss these bonding orbitals, we will first examine frontier orbitals of the 1-silaallyl group,  $\cdot\text{H}_2\text{SiCHCH}_2$ , and the usual allyl group,  $\cdot\text{H}_2\text{CCHCH}_2$  (see Figure 6A,B). The SOMO of both  $\cdot\text{H}_2\text{SiCHCH}_2$  and  $\cdot\text{H}_2\text{CCHCH}_2$  is a nonbonding  $\pi$  orbital ( $\varphi_{\text{n}\pi}$ ), which consists of p orbitals of terminal C2 and Si (or C3) atoms. It is noted that  $\varphi_{\text{n}\pi}$  of  $\cdot\text{H}_2\text{SiCHCH}_2$  is much

different from that of  $\cdot\text{H}_2\text{CCHCH}_2$ , as follows:  $\varphi_{\text{n}\pi}$  of  $\cdot\text{H}_2\text{CCHCH}_2$  is symmetrical; in other words, the p orbitals of terminal C atoms contribute to  $\varphi_{\text{n}\pi}$  to the same extent (Figure 6A). On the other hand, the p orbital of Si contributes more to  $\varphi_{\text{n}\pi}$  than that of terminal C2 in  $\cdot\text{H}_2\text{SiCHCH}_2$  (Figure 6B). This is because the p orbital of  $\cdot\text{SiH}_3$  is at much higher energy ( $-5.39$  eV) than that of  $\cdot\text{CH}_3$  ( $-6.41$  eV), where orbital energies are calculated with the DFT/BS-II method; note that Hartree–Fock orbitals show similar energy differences between them.<sup>23</sup> The  $\varphi_{\text{n}\pi}$  orbitals of  $\cdot\text{H}_2\text{SiCHCH}_2$  and  $\cdot\text{H}_2\text{CCHCH}_2$  overlap with the SOMO of  $\cdot\text{Cp}(\text{CO})_2\text{W}$  (Figure 6D) in a bonding way to form the HOMO – 2 of **1** and **1C**. Because the Si p orbital contributes more to  $\varphi_{\text{n}\pi}$  than the C p orbital, the W–Si overlap is much larger than the W–C2 overlap in the HOMO – 2 of **1**. On the other hand, the W–C2 overlap is the same as the W–C3 overlap in the HOMO – 2 of **1C**.

The HOMO – 1 of both  $\cdot\text{H}_2\text{SiCHCH}_2$  and  $\cdot\text{H}_2\text{CCHCH}_2$  is a bonding  $\pi$  orbital ( $\varphi_{\pi}$ ), but a significantly large difference is observed between them, as follows: The p orbitals of all three C atoms contribute to  $\varphi_{\pi}$ , and therefore,  $\varphi_{\pi}$  is well delocalized in  $\cdot\text{H}_2\text{CCHCH}_2$  (Figure 6A). On the other hand, the p orbital of Si contributes much less to  $\varphi_{\pi}$  than that of C3 (Figure 6B). As a result, the conjugation between the Si and C atoms is very weak in  $\varphi_{\pi}$  of  $\cdot\text{H}_2\text{SiCHCH}_2$ . This is interpreted in terms of orbital energy and orbital overlap; because  $\varphi_{\text{n}\pi}$  is at much higher energy than  $\varphi_{\pi}$  and the Si p orbital is at much higher energy than that of C, as described above, the Si p orbital contributes much more to  $\varphi_{\text{n}\pi}$  but much less to  $\varphi_{\pi}$  than that of C. Also, the longer Si–C bond distance than the C–C distance leads to smaller overlap between the Si p and C p orbitals. Certainly, the Laplacian of the electron density shows much smaller conjugation between the Si and C1 atoms in **1** than that between the C1 and C3 atoms in **1C**, as discussed above. This  $\varphi_{\pi}$  orbital of  $\cdot\text{H}_2\text{SiCHCH}_2$  and  $\cdot\text{H}_2\text{CCHCH}_2$  overlaps with the acceptor orbital (LUMO) of  $\cdot\text{Cp}(\text{CO})_2\text{W}$  (Figure 6D) in a bonding way to form the HOMO – 5 of **1** and **1C**. Because the  $\pi$  orbital of the C=C double bond contributes much more to  $\varphi_{\pi}$  of  $\cdot\text{H}_2\text{SiCHCH}_2$  than the Si p orbital, the HOMO – 5 of **1** is considerably different from that of **1C**, as shown in Figure 5.

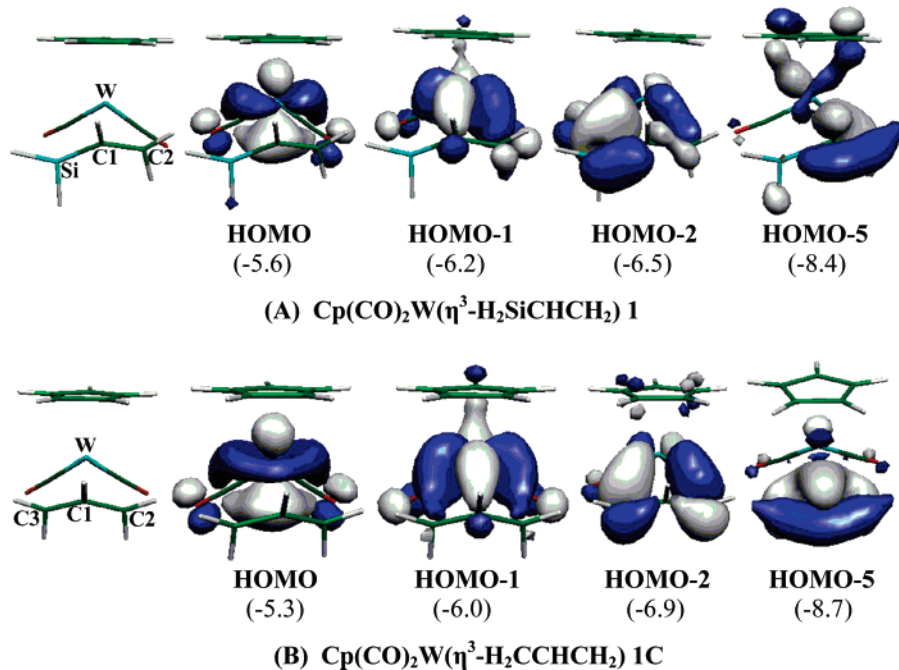


**Figure 5.** Several important Kohn–Sham orbitals in **1** and **1C**. Kohn–Sham orbital energies (eV) are given in parentheses.

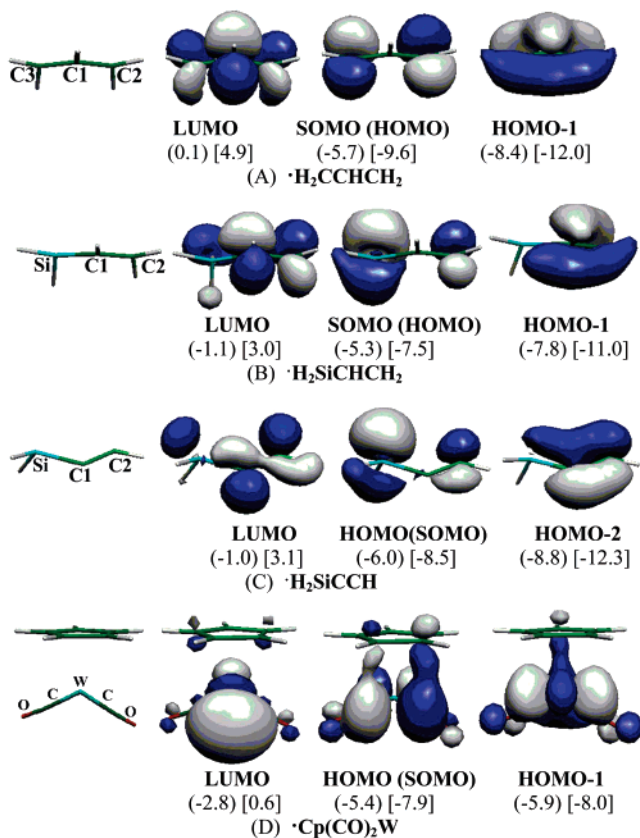


**Figure 6.** Several important Kohn–Sham orbitals in the fragments  $\cdot\text{H}_2\text{CCHCH}_2$ ,  $\cdot\text{H}_2\text{SiCHCH}_2$ ,  $\cdot\text{H}_2\text{SiCCH}$ , and  $\cdot\text{Cp}(\text{CO})_2\text{W}$ . Kohn–Sham and HF orbital energies (eV) are given in parentheses and brackets, respectively.

Apparently, the HOMO – 5 of **1** mainly contains the coordinate bond of the C=C double bond with the empty d orbital of W. On the other hand,  $\varphi_\pi$  of  $\cdot\text{H}_2\text{CCHCH}_2$  interacts with the empty d orbital of W in **1C** to form the delocalized bonding interaction between the W center and three C atoms. In conclusion,  $\eta^3\text{-H}_2\text{SiCHCH}_2$  interacts with the W center through the coordinate bonds of the C=C  $\pi$  orbital and Si p orbital with the LUMO of  $\text{Cp}(\text{CO})_2\text{W}$  in **1**, while  $\eta^3\text{-H}_2\text{CCHCH}_2$  interacts with the W center through the coordinate bonds of delocalized  $\varphi_{\pi\pi}$  and  $\varphi_\pi$  orbitals with the LUMO of  $\text{Cp}(\text{CO})_2\text{W}$  in **1C**. These results are consistent with the Laplacian plots of **1** and **1C**, as discussed above.

The HOMO – 1 of **1C** consists of the bonding overlap between the  $\pi^*$  orbital ( $\varphi_{\pi^*}$ ) of the  $\eta^3$ -allyl group and the HOMO – 1 of  $\cdot\text{Cp}(\text{CO})_2\text{W}$ . This is a typical  $\pi$ -back-donation interaction. On the other hand, the  $\pi$ -back-donation of **1** is much different from that of **1C**, as follows: The Si p orbital contributes little to the HOMO – 1 of **1**. This is because the Si p orbital largely contributes to  $\varphi_{\pi\pi}$  of  $\cdot\text{H}_2\text{SiCHCH}_2$  but little to  $\varphi_{\pi^*}$  of  $\cdot\text{H}_2\text{SiCHCH}_2$  (Figure 6B). Thus, the HOMO – 1 of **1** is understood in terms of the  $\pi$ -back-donation from the occupied d orbital of W to the  $\pi^*$  orbital of the C=C double bond.

These features relate to the geometry of **1** as follows: The Si–C1 (1.826 Å) and C1–C2 (1.425 Å) bond distances in **1** are intermediate between the Si–C single and Si=C double bonds and between the C–C single and C=C double bonds, respectively;  $R(\text{Si–C}) = 1.895$  Å,  $R(\text{Si=C}) = 1.717$  Å,  $R(\text{C=C}) = 1.542$  Å, and  $R(\text{C=C}) = 1.334$  Å, where the DFT/BS-I-optimized values are presented.<sup>24</sup>

From these results, the following conclusions are presented: (1) The Si p orbital contributes more to  $\varphi_{\pi\pi}$  than the C p orbital.

(2) The Si p orbital contributes little to  $\varphi_\pi$ , indicating that  $\varphi_\pi$  is understood in terms of the  $\pi$  orbital between two C atoms. (3) As a result, the  $\pi$ -conjugation between Si and C atoms is much smaller than that of the  $\eta^3$ -allyl group. (4) Complex **1** is understood to be a species between  $\eta^3$ -vinylsilyl and  $\eta^3$ -1-silaallyl complexes. (5) These features arise from the fact that the p orbital of Si is at higher energy than that of C and the Si–C distance is longer than the C–C distance.

**Geometry and Bonding Nature of 2.**  $\text{Cp}(\text{CO})_2\text{W}(\text{CHCH}_2)(\text{SiH}_2)$  **4** is understood to be a tungsten acetylidy silylene complex in which charge transfer (CT) occurs from the  $\pi$  orbital of the acetylidy moiety to the empty p orbital of the silylene and simultaneously the reverse CT occurs from the  $\text{sp}^2$  lone pair orbital of the silylene to the  $\pi^*$  orbital of the acetylidy.<sup>7</sup> Though similar bonding interactions are expected in **2**, several differences are observed between **2** and **4**, as follows: The W–C1, Si–C1, and Si–C2 distances in **2** are significantly longer than those of **4** by 0.183, 0.079, and 0.393 Å, respectively (see Figure 1 and ref 7 for the optimized geometries of **2** and **4**, respectively). The longer W–C1 bond of **2** suggests that the W–vinyl bond in **2** is weaker than the W–acetylidy bond in **4**. The significantly longer Si–C1 and Si–C2 distances of **2** suggest that the interaction between the silylene and vinyl groups is much weaker in **2** than that between the silylene and acetylidy groups in **4**. On the other hand, the W–Si distance in **2** is significantly shorter than that of **4**, indicating that the W–silylene interaction is stronger in **2** than in **4**. Consistent with these geometrical features, the  $\text{sp}^2$  lone pair orbital of silylene expands toward the W center at a small angle of 7.5° with the W–Si bond and at a large angle of 50.2° with the Si–C1 bond in **2**. On the other hand, its direction considerably shifts toward the C1 atom from the W center in **4**; the lone pair orbital makes a considerably large angle of 35.4° with the W–Si bond and a considerably small angle of 14.3° with the Si–C1 bond. It is worth investigating the reasons why the geometry of **2** is much different from that of **4**, because these features deeply relate to the reason why **2** cannot be isolated.

The Laplacian plots on the Si–C1–C2 plane clearly show that the electron accumulation between the silylene and vinyl groups in **2** is smaller than that between the silylene and acetylidy groups in **4** (Figure 7). These results indicate that the interaction between the silylene and vinyl groups in **2** is weaker than that between the silylene and acetylidy groups in **4**. The Laplacian plot on the W–Si–C1 plane (Figure 8) shows that the electron accumulation between the W center and silylene is larger in **2** than in **4**, indicating that the W–silylene bond is stronger in **2** than in **4**. Also, the electron accumulation between the W center and the acetylidy group in **4** is larger than that between the W center and the vinyl group in **2** (Figure 8). This result suggests that the W–acetylidy interaction in **4** is stronger than the W–vinyl interaction in **2**.

The HOMO and HOMO – 1 of **2** mainly consist of a W d orbital. The presence of these two doubly occupied d orbitals is consistent with the +2 oxidation state of W (d<sup>4</sup> system). The HOMO – 2 and HOMO – 7 include the bonding interactions of the W center with the silylene and vinyl groups, as shown in Figure 9. Both are somewhat different from the corresponding HOMO – 2 and HOMO – 6 of **4** (see ref 7 for the orbital pictures of **4**). The HOMO – 2 of **2** mainly consists of the bonding overlap between the empty d orbital of W and the  $\text{sp}^2$

(23) The HF-calculated p orbital of  $\cdot\text{SiH}_3$  is at –7.85 eV, and that of  $\cdot\text{CH}_3$  is at –10.47 eV.

(24) DFT(B3PW91)/BS-I-optimized geometries of  $\text{H}_3\text{Si–CH}_3$ ,  $\text{H}_2\text{Si=CH}_2$ ,  $\text{CH}_3\text{–CH}_3$ , and  $\text{CH}_2=\text{CH}_2$  were taken, respectively.

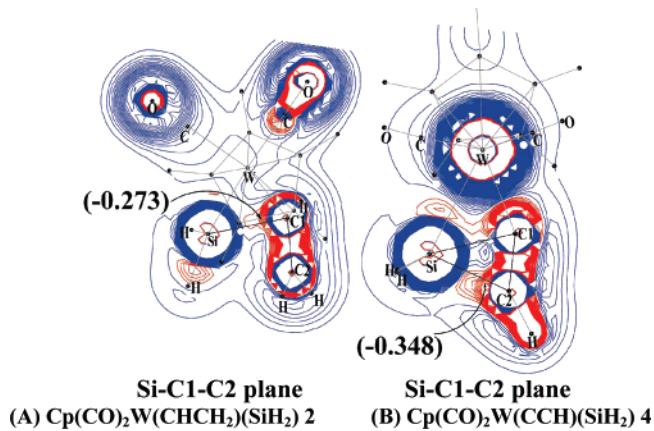


**Figure 7.** Laplacian of the electron density on the Si–C1–C2 plane of **2** and **4**. Contour values are 0.0,  $\pm 0.025$ ,  $\pm 0.05$ , .... Red and blue lines represent accumulation of electron density and depletion of electron density, respectively. Values (au) in the negative region are given in parentheses.

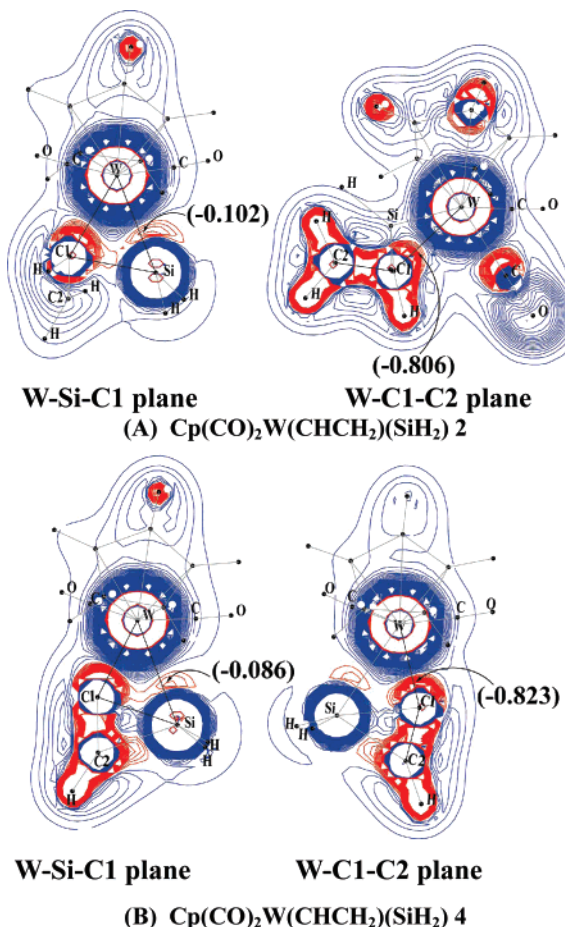


**Figure 8.** Laplacian of the electron density on the W–Si–C1 and W–C1–C2 planes of **2** and **4**. Contour values are 0.0,  $\pm 0.025$ ,  $\pm 0.050$ , .... Red and blue lines represent accumulation of electron density and depletion of electron density, respectively. Values (au) in the negative region are given in parentheses.

lone pair orbital of silylene. However, bonding interaction is little observed between the silylene and vinyl groups in this HOMO – 2, while considerably large bonding overlap between the silylene and acetylidy groups is observed in the HOMO – 2 of **4**. This significant difference in the HOMO – 2 between **2** and **4** is consistent with the much smaller accumulation of electron density between the silylene and vinyl groups in **2** than

that between the silylene and acetylidy groups in **4**, as described above and in Figure 7. Moreover, the  $sp^2$  lone pair orbital of silylene expands outside the W–Si–C1 triangle in **2**, unlike that of **4**. In the HOMO – 7 of **2**, bonding overlap is observed between the Si and C1 atoms, while its position is different from those of both the  $sp^2$  lone pair and empty p orbitals of silylene. These features of the HOMO – 2 and HOMO – 7 are interpreted in terms of orbital interactions among the  $sp^2$  lone pair and empty p orbitals of the silylene group and the  $sp^2$  lone pair orbital of the vinyl group as follows: The  $sp^2$  lone pair orbital of the silylene overlaps with the  $sp^2$  lone pair orbital of the vinyl group in an antibonding way. Into this antibonding overlap, the empty p orbital of the silylene mixes in a bonding way with the  $sp^2$  lone pair orbital of the vinyl group, as shown in Scheme 3A, because the empty p orbital of the silylene is at higher energy than the antibonding overlap; the  $sp^2$  lone pair and empty p orbitals of SiH<sub>2</sub> are at –6.2 and –3.2 eV, respectively, and the  $sp^2$  lone pair of  $^3\text{CHCH}_2$  is at –7.9 eV, where the Kohn–Sham orbital energies are presented.<sup>25</sup> These orbital mixings lead to formation of the HOMO – 2. In the bonding counterpart of the HOMO – 2, the  $sp^2$  lone pair orbital of the vinyl group overlaps with the  $sp^2$  lone pair orbital of the silylene in a bonding way, into which the empty p orbital of the silylene mixes in a bonding way, as shown in Scheme 3B, because the empty p orbital of silylene is at higher energy than the  $sp^2$  lone pair orbitals of the vinyl and silylene groups. These orbital mixings lead to formation of the HOMO – 7. In other words, in **2**, the  $sp^2$  lone pair orbital of the vinyl group participates in the CT interaction with the silylene group, whereas the  $\pi$  orbital of the vinyl group participates little in the CT with the silylene. In **4**, on the other hand, both the  $\pi$  and  $\pi^*$  orbitals of the acetylidy group participate in the CT interaction with the silylene group, as discussed previously.<sup>7</sup> The reason for these significant differences between **2** and **4** can be understood in terms of the differences in geometry between the vinyl and acetylidy groups, which will be discussed below.

From the above-discussed geometrical features, the Laplacian of the electron density, and orbital pictures, it is clearly concluded that **2** can be understood as a tungsten vinyl silylene complex in which the CT interaction between the vinyl and silylene groups is weak.

**Relative Stabilities of 1 and 2 and Conversion Reaction of 1 to 2.** Before discussing the relative stabilities and the activation barrier of the conversion reaction of **1** to **2**, we examine briefly what computational method presents reliable results of the energy change. The CCSD(T) and DFT methods present similar activation barriers, as shown in Table 2, while the MP4(SDTQ) method presents a moderately larger activation barrier than the CCSD(T) and DFT methods; see Supporting Information Table S1 for MP2- to MP4(SDTQ)-calculated values. Moreover, the barrier moderately fluctuates around the MP2 and MP3 levels and somewhat increases upon going to the MP4(SDTQ) level from the MP4(SDQ) level. The reaction energy depends much less on the computational methods, while the MP4(SDTQ) method presents a larger reaction energy than the CCSD(T) and DFT methods. In the conversion reaction of **3** to **4**, the MP4(SDQ), MP4(SDTQ), and CCSD(T) methods present similar reaction energies, while the DFT method presents a moderately larger exothermicity than the others.<sup>7</sup> From these results, it is concluded that the CCSD(T) method presents

(25) The geometries of the silylene and vinyl groups were taken to be the same as those in **2**.

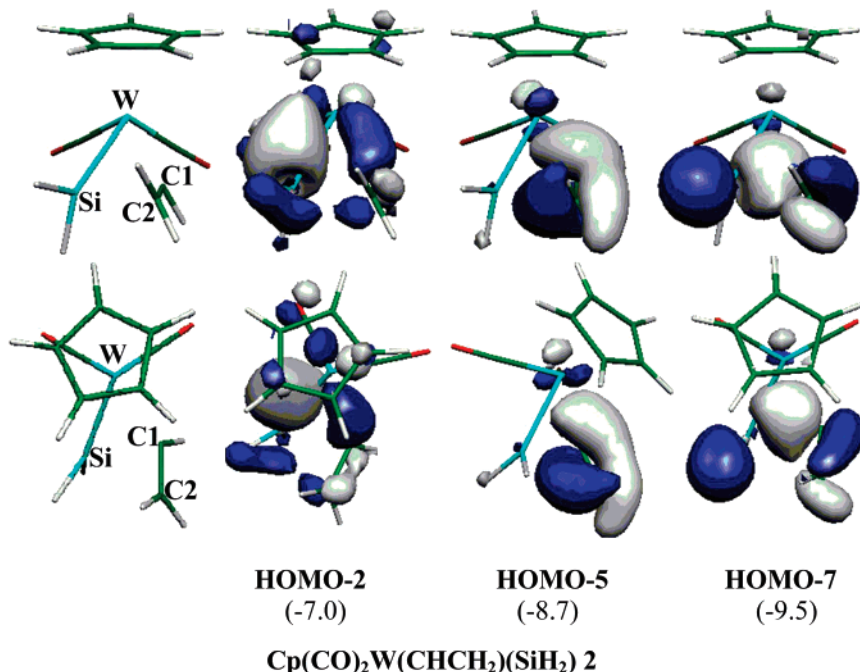


**Figure 9.** Several important Kohn-Sham orbitals in **2**. In parentheses are the orbital energies (eV).

**Scheme 3**

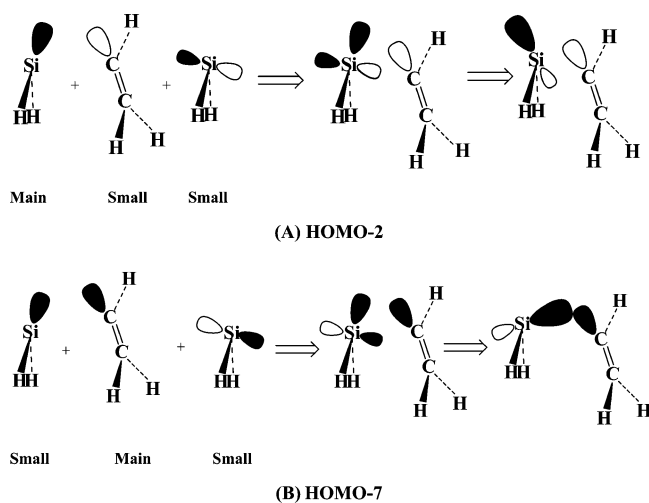


**Table 2. Activation Barriers ( $E_a$ )<sup>a</sup> and Reaction Energies ( $\Delta E$ )<sup>a</sup> of the Conversion Reactions of **1** to **2** and of **3** to **4****

method <sup>c</sup>	conversion reaction of <b>1</b> to <b>2</b>		conversion reaction of <b>3</b> to <b>4</b> <sup>b</sup>	
	$E_a$ (kcal/mol)	$\Delta E$ (kcal/mol)	$E_a$ (kcal/mol)	$\Delta E$ (kcal/mol)
DFT	33.2	20.9	15.3	-4.9
CCSD(T)	34.2	21.0	15.8	-0.7

<sup>a</sup>  $E_a$  is the energy difference between the transition state and the reactant, and  $\Delta E$  is the energy difference between the product and the reactant. BS-II was employed. <sup>b</sup> Reference 7. <sup>c</sup> See Supporting Information Table S1 for MP4(SDTQ)-calculated values.

reliable results. Here, we present a discussion based on the CCSD(T)- and DFT-calculated values.

Complex **1** converts to **2** with a large endothermicity of 21.0 (20.9) kcal/mol (see Table 2), where the CCSD(T)- and DFT-calculated values are given without and in parentheses, respectively, hereafter. On the other hand, **3** converts to **4** with a moderate exothermicity of 0.7 (4.9) kcal/mol (Table 2). These results clearly indicate that **1** is much more stable than **2** but **3** is moderately less stable than **4**. Consistent with these results

of the relative stabilities, the tungsten  $\eta^3$ -1-silaallyl/ $\eta^3$ -vinylsilyl complex was isolated experimentally but the similar tungsten  $\eta^3$ -1-silapropargyl/ $\eta^3$ -alkynylsilyl complex was not, while the tungsten acetylide silylene complex was isolated experimentally but the similar tungsten vinyl silylene complex was not.

It is very important to clarify whether **1** easily converts to **2**. This reaction takes place via  $\alpha$ -Si—C  $\sigma$ -bond activation like the conversion reaction of **3** to **4**.<sup>7</sup> Apparently, the geometry changes by the conversion reaction of **1** to **2** are similar to those of **3** to **4**,<sup>7</sup> as shown in Figure 1. Thus, we mention only important geometrical changes here. Upon going to the transition state **TS**<sub>1-2</sub> from **1**, the Si—C1 distance moderately lengthens to 1.907 Å by 0.081 Å and the C1—C2 distance moderately shortens to 1.348 Å by 0.077 Å. Significantly large changes are observed in the orientation of the C1—C2 bond and the W—C2 distance. The direction of the  $sp^2$  orbital of the CH=CH<sub>2</sub> group changes much more toward the W center in **TS**<sub>1-2</sub> than that of the  $sp$  orbital of the C≡CH group in **TS**<sub>3-4</sub>; the WC1C2 angle increases by 77.7° upon going to **TS**<sub>1-2</sub> from **1**, but it increases by 58.9° upon going to **TS**<sub>3-4</sub> from **3**. This direction change induces the considerably large lengthening of the W—C2 bond in **TS**<sub>1-2</sub>. Also, the W—C1 bond considerably lengthens by 0.274 Å upon going to **TS**<sub>1-2</sub> from **1**, which is in contrast with the slight decrease of the W—C1 bond by 0.055 Å upon going to **TS**<sub>3-4</sub> from **3**.

The activation barrier of the conversion reaction of **1** to **2** is calculated to be 34.2 (33.2) kcal/mol (see Table 2), while that of the conversion reaction of **3** to **4** is moderate, being 15.8 (15.3) kcal/mol.<sup>7</sup> These results indicate that the tungsten  $\eta^3$ -silaallyl/ $\eta^3$ -vinylsilyl complex **1** is stable, unlike the tungsten  $\eta^3$ -silapropargyl/ $\eta^3$ -alkynylsilyl complex **3**. The origin of the large activation barrier of the conversion reaction of **1** to **2** is easily understood by inspecting the geometry changes in **TS**<sub>1-2</sub> and the bonding interactions of **1**. The C=C double bond coordinates with the W center in **1**, as discussed above, and the coordinate bond is much stronger in **1** than in **3**, which will be discussed below. We already found that the W—C2 bond lengthens much more and the W—C1 bond lengthens moderately more in **TS**<sub>1-2</sub> than in **TS**<sub>3-4</sub>. These geometry changes suggest

**Table 3. Interaction Energies (INT) Calculated between the H<sub>2</sub>SiCHCH<sub>2</sub> and Cp(CO)<sub>2</sub>W Moieties in **1** and between the H<sub>2</sub>SiCCH and Cp(CO)<sub>2</sub>W Moieties in **3****

method <sup>b</sup>	INT <sup>a</sup> (kcal/mol)	
	<b>1</b>	<b>3</b>
DFT	110.3	102.0
CCSD(T)	122.1	112.7

<sup>a</sup> INT =  $E_t(\mathbf{1} \text{ or } \mathbf{3}) - E_t[\text{Cp}(\text{CO})_2\text{W}] - E_t[\text{H}_2\text{SiCHCH}_2 \text{ or } \text{H}_2\text{SiCCH}]$ . BS-II was employed. <sup>b</sup> See Supporting Information Table S2 for MP4(SDTQ)-calculated values.

that the coordinate bond of the C=C double bond with the W center is almost broken in **TS<sub>1-2</sub>**. This bond breaking induces a larger energy loss in **TS<sub>1-2</sub>** than in **TS<sub>3-4</sub>**. As a result, the conversion reaction of **1** to **2** needs a larger activation barrier than that of **3** to **4**.

**Reasons Why **1** Is Isolated but **3** Is Not and Why **4** Is Isolated but **2** Is Not.** In the conversion reaction of **1** to **2**, the bonding interaction between the Cp(CO)<sub>2</sub>W and  $\eta^3$ -silaallyl/ $\eta^3$ -vinylsilyl groups and the Si–C bond are broken. The interaction energy between the Cp(CO)<sub>2</sub>W and H<sub>2</sub>SiCHCH<sub>2</sub> moieties is calculated with various methods, as shown in Table 3. Though the MP4(SDQ)- and MP4(SDTQ)-calculated values are considerably larger than the DFT- and CCSD(T)-calculated values (MP4(SDTQ)-calculated values are given in Supporting Information Table S2), the CCSD(T)-calculated value is moderately larger than the DFT-calculated value. However, their differences between **1** and **3** are similar in the DFT and CCSD(T) methods. Thus, we believe that a reliable discussion can be presented based on DFT- and CCSD(T)-calculated values. This interaction energy in **1** is larger than the interaction energy between the Cp(CO)<sub>2</sub>W and H<sub>2</sub>SiCCH moieties in **3** by 9.4 (8.3) kcal/mol (see Table 3). The reason is easily understood, as follows: The SOMOs of H<sub>2</sub>SiCHCH<sub>2</sub> and H<sub>2</sub>SiCCH are the  $\varphi_{\pi\pi}$  orbitals, which overlap with the d orbital (SOMO) of W to form the HOMO – 2 of both **1** and **3** (see Figure 5A and Supporting Information Figure S1 for orbital pictures of **1** and **3**, respectively). The SOMO (–5.3 eV) of H<sub>2</sub>SiCHCH<sub>2</sub> is at moderately higher energy than that (–6.0 eV) of H<sub>2</sub>SiCCH, where the Kohn–Sham orbital energies are presented (see Figure 6B,C). The SOMO of Cp(CO)<sub>2</sub>W is at an energy of –5.4 eV, which is between the SOMO energies of H<sub>2</sub>SiCHCH<sub>2</sub> and H<sub>2</sub>SiCCH (see Figure 6D). The covalent bond energy  $\Delta E_{\text{cov}}$  is approximately represented by eq 1,

$$\Delta E_{\text{cov}} = |\epsilon_A - \epsilon_B| + \beta^2/|\epsilon_A - \epsilon_B| \quad (1)$$

where  $\epsilon_A$  and  $\epsilon_B$  are the orbital energies of the SOMOs and  $\beta$  is the resonance integral. Equation 1 indicates that the covalent bond energy increases with an increase in the energy difference between two SOMOs. Because the energy difference between the SOMOs of H<sub>2</sub>SiCHCH<sub>2</sub> and Cp(CO)<sub>2</sub>W is not very different from that between the SOMOs of H<sub>2</sub>SiCCH and Cp(CO)<sub>2</sub>W, it is likely that the W–Si bond energies are similar in **1** and **3**. The HOMO – 1 of H<sub>2</sub>SiCHCH<sub>2</sub> and the HOMO – 2 of H<sub>2</sub>SiCCH are the  $\varphi_{\pi}$  orbitals, which overlap with the empty d orbital (LUMO) of Cp(CO)<sub>2</sub>W in a bonding way to form the HOMO – 5 of **1** and the HOMO – 7 of **3**, as discussed above. Because this is a CT interaction and the  $\varphi_{\pi}$  orbital (–7.8 eV) of H<sub>2</sub>SiCHCH<sub>2</sub> is at higher energy than that of H<sub>2</sub>SiCCH (–8.8 eV), the W–(C=C) coordinate bond of **1** is stronger than the W–(C≡C) coordinate bond of **3**. The HOMO – 1 mainly includes the  $\pi$ -back-donation interaction in **1** and **3**. This is formed by CT from the doubly occupied d orbitals (HOMO – 1) of Cp(CO)<sub>2</sub>W to the  $\pi^*$  orbitals of H<sub>2</sub>SiCHCH<sub>2</sub> and H<sub>2</sub>SiCCH.

**Table 4. Si–C Bond Energies (E<sub>Si–C</sub>) in H<sub>3</sub>SiCHCH<sub>2</sub> and H<sub>3</sub>SiCCH<sup>a</sup>**

method <sup>c</sup>	E <sub>Si–C</sub> <sup>b</sup> (kcal/mol)	
	H <sub>3</sub> SiCHCH <sub>2</sub>	H <sub>3</sub> SiCCH
DFT	50.6	86.4
CCSD(T)	46.8	83.3

<sup>a</sup> The geometries are the same as those in **1** and **3** (see Supporting Information Figure S2 for the geometries). <sup>b</sup> E<sub>Si–C</sub> =  $E_t(\text{H}_3\text{SiCHCH}_2 \text{ or } \text{H}_3\text{SiCCH}) - E_t(\text{SiH}_3) - E_t(\text{CHCH}_2 \text{ or } \text{CCH})$ . <sup>c</sup> See Supporting Information Table S3 for MP4(SDTQ)-calculated values.

SiCCH. The LUMO (–1.1 eV) of H<sub>2</sub>SiCHCH<sub>2</sub> is at an energy similar to that (–1.0 eV) of H<sub>2</sub>SiCCH (see Figure 6B,C). Thus, the  $\pi$ -back-donation contributes similarly to the coordinate bonds of **1** and **3**. From these results, it is concluded that the stronger CT from the  $\pi$  orbital of vinyl to the d orbital of W is responsible for the stronger interaction between the Cp(CO)<sub>2</sub>W and H<sub>2</sub>SiCHCH<sub>2</sub> moieties than that between the Cp(CO)<sub>2</sub>W and H<sub>2</sub>SiCCH moieties.

On the other hand, the Si–C bond is considerably stronger in H<sub>3</sub>SiCCH by 36.5 (35.8) kcal/mol than in H<sub>3</sub>SiCHCH<sub>2</sub> (see Table 4 and Supporting Information Table S3), where the geometries of H<sub>3</sub>SiCCH and H<sub>3</sub>SiCHCH<sub>2</sub> were taken to be the same as those of **1** and **3**.<sup>26</sup> This is easily interpreted in terms of the SOMO energies of CHCH<sub>2</sub> (sp<sup>2</sup> lone pair orbital) and CCH (sp lone pair orbital). The SOMO (–7.7 eV) of CHCH<sub>2</sub> is at much higher energy than that (–10.1 eV) of CCH, where the Kohn–Sham orbital energies are presented.<sup>27</sup> The SOMO of SiH<sub>3</sub> is at –5.5 eV.<sup>27</sup> Because the energy difference in SOMOs between CHCH<sub>2</sub> and SiH<sub>3</sub> is considerably smaller than that between CCH and SiH<sub>3</sub>, the Si–C bond is considerably weaker in H<sub>3</sub>SiCHCH<sub>2</sub> than that of H<sub>3</sub>SiCCH; see eq 1.

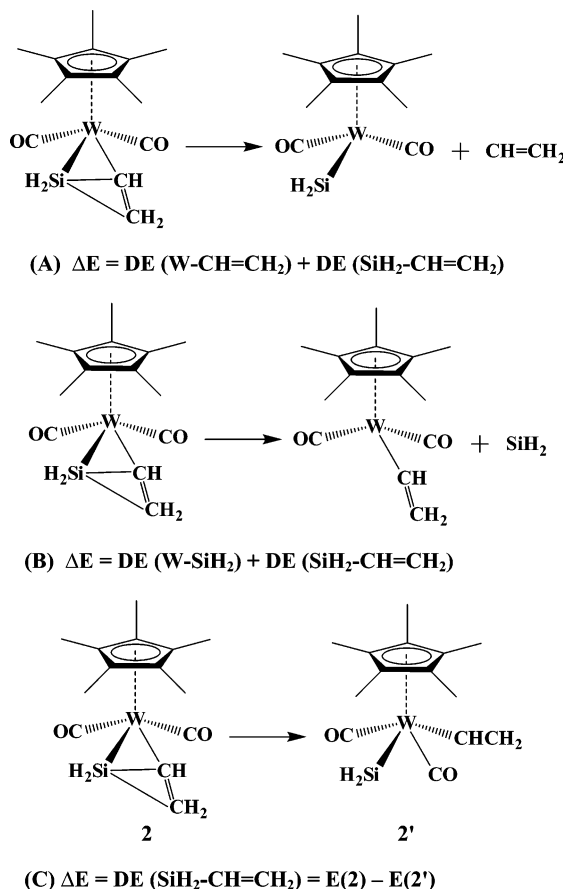
The W–silylene and W–acetylido interactions in **4** are very different from the usual W–silylene and W–acetylido bonds, because a considerably strong silylene–acetylido interaction is formed in **4**. Thus, we evaluated the W–silylene, W–vinyl, and silylene–vinyl interaction energies in **2** and the W–silylene, W–acetylido, and silylene–acetylido interaction energies in **4** in an approximate manner, as shown in Scheme 4; for instance, when the vinyl moiety is eliminated from **2**, the W–vinyl and silylene–vinyl interactions are broken. Thus, the energy loss corresponds to the sum of the W–vinyl and silylene–vinyl bonding interactions, as shown in Scheme 4A. The silylene–vinyl interaction was evaluated as the energy difference between **2** and **2'**, as shown in Scheme 4C, where the geometry of **2'** was taken to be the same as that of **2** except for the positions of the CO and CHCH<sub>2</sub> groups; their positions were exchanged with each other so as not to allow the CHCH<sub>2</sub> group to interact with the SiH<sub>2</sub> group. The energy difference between **2** and **2'** corresponds to the silylene–vinyl interaction. These values are summarized in Table 5 (see Supporting Information Table S4 for MP4(SDTQ)-calculated values).

The W–silylene bond of **2** is stronger than that of **4** by 5.0 (5.9) kcal/mol, which is consistent with the above discussion based on the Laplacian of the electron density. This is because the sp<sup>2</sup> lone pair orbital of silylene expands toward the W center in **2** but its direction changes toward the C1 atom in **4**, as we discussed previously;<sup>7</sup> in other words, the sp<sup>2</sup> lone pair of the

(26) In both H<sub>3</sub>SiCHCH<sub>2</sub> and H<sub>3</sub>SiCCH, the third H atom connected with Si was placed on the W–Si bond line of **1** and **3**, respectively, with the usual Si–H distance (1.490 Å); see Supporting Information Figure S2A for the geometries.

(27) The geometries of SiH<sub>3</sub>, CHCH<sub>2</sub>, and CCH were taken to be the same as those in **1** and **3**; see Supporting Information Figure S2B for the geometries.

Scheme 4

Table 5. W–Silylene, W–Vinyl, and Silylene–Vinyl Bond Energies (DE)<sup>a</sup> in 2 and W–Silylene, W–Acetylido, and Silylene–Acetylido Bond Energies (DE)<sup>a</sup> in 4

method <sup>b</sup>	DE (kcal/mol) in 2			DE (kcal/mol) in 4		
	W–SiH <sub>2</sub>	W–CH <sub>2</sub> CH <sub>2</sub>	SiH <sub>2</sub> –CHCH <sub>2</sub>	W–SiH <sub>2</sub>	W–CCH	SiH <sub>2</sub> –CCH
DFT	39.9	43.6	47.4	34.0	88.8	74.6
CCSD(T)	42.0	50.2	43.0	37.0	77.0	64.9

<sup>a</sup> See Scheme 4 for the DE calculation method. BS-II was employed.  
<sup>b</sup> See Supporting Information Table S4 for MP4(SDTQ)-calculated values.

silylene overlaps better with the empty d orbital of W in **2** than in **4**. The W–vinyl bond of **2** is considerably weaker than the W–acetylido bond of **4** by 26.8 (45.2) kcal/mol. The silylene–acetylido interaction is much stronger than the silylene–vinyl interaction by 21.9 (27.2) kcal/mol. These results are also consistent with results of the Laplacian of the electron density. The reason will be discussed below in more detail. As shown in Scheme 5, the sum of the W–(η<sup>3</sup>-H<sub>2</sub>SiCHCH<sub>2</sub>) and Si–C bond energies in **1** is larger than that of the W–vinyl, W–silylene, and silylene–vinyl interaction energies in **2** by 33.7 (30.0) kcal/mol. Interestingly, this energy difference is similar to the endothermicity of the conversion reaction of **1** to **2**, suggesting that the bond energies evaluated here are reliable. On the other hand, the sum of the W–(η<sup>3</sup>-H<sub>2</sub>SiCCH) and Si–C bond energies in **3** is smaller than that of the W–acetylido, W–silylene, and silylene–acetylido interaction energies in **4** by 9.0 kcal/mol, where the DFT-calculated values were adopted. In the CCSD(T) calculations, the sum of the W–(η<sup>3</sup>-H<sub>2</sub>SiCCH) and Si–C bond energies in **3** is larger than that of the W–acetylido, W–silylene, and silylene–acetylido interaction energies in **4** by 17.1 kcal/mol. Though this energy difference is the reverse of the relative stabilities of **3** and **4**, the CCSD-

Scheme 5

Cp(CO) <sub>2</sub> W(η <sup>3</sup> -H <sub>2</sub> SiCHCH <sub>2</sub> ) <b>1</b>	→	Cp(CO) <sub>2</sub> W(CHCH <sub>2</sub> )(SiH <sub>2</sub> ) <b>2</b>
W–(η <sup>3</sup> -H <sub>2</sub> SiCHCH <sub>2</sub> ): 122.1 (110.3)	W–vinyl:	50.2 (43.6)
Si–C: 46.8 (50.6)	W–silylene:	42.0 (39.9)
Total: 168.9 (160.9)	Silylene–vinyl:	43.0 (47.4)
	Total:	135.2 (130.9)
	Difference =	+ 33.7 (30.0)
Cp(CO) <sub>2</sub> W(η <sup>3</sup> -H <sub>2</sub> SiCCH) <b>3</b>	→	Cp(CO) <sub>2</sub> W(CCH)(SiH <sub>2</sub> ) <b>4</b>
W–(η <sup>3</sup> -H <sub>2</sub> SiCCH): 112.7 (102.0)	W–acetylido:	77.0 (88.8)
Si–C: 83.3 (86.4)	W–silylene:	37.0 (34.0)
Total: 196.0 (188.4)	Silylene–acetylido:	64.9 (74.6)
	Total:	178.9 (197.4)
	Difference =	+ 17.1 (-9.0)

CCSD(T)/BS-II and DFT/BSII-calculated values (in kcal/mol unit) are presented without and in parenthesis, respectively.

(T)-calculated energy difference between **3** and **4** is much smaller than that between **1** and **2**. Thus, it is concluded that **3** is less easily isolated than **1** even if we take the CCSD(T)-calculated energy changes.

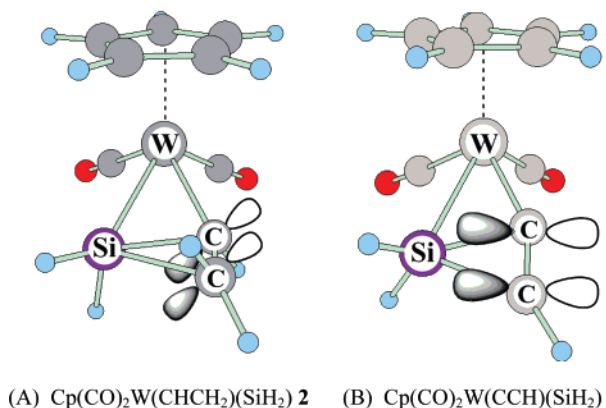
From these results, we can easily understand the reasons why **1** was isolated but **2** was not. Though the Si–C bond is weak in **1**, the W–(η<sup>3</sup>-H<sub>2</sub>SiCHCH<sub>2</sub>) interaction is considerably strong. Moreover, the W–vinyl and silylene–vinyl interactions are very weak in **2**. As a result, **1** was isolated but **2** was not. On the other hand, the Si–C bond is strong in **3** but the W–(η<sup>3</sup>-H<sub>2</sub>SiCCH) interaction is weak. Moreover, the W–acetylido and silylene–acetylido interactions are very strong in **4**. As a result, **4** was isolated but **3** was not.

**Reasons Why the W–Acetylido Bond Is Stronger Than the W–Vinyl Bond.** It is of considerable interest to clarify the reasons why the W–acetylido bond is stronger than the W–vinyl bond, because this is one of the important factors in stabilizing **4** relative to **3**. We also evaluated the W–vinyl bond energy in an ideal complex, **5** (Figure 2), in which the vinyl group was placed at the side opposite the silylene to evaluate the pure W–vinyl bond energy. Also, the pure W–acetylido bond energy was calculated from the similar ideal complex Cp(CO)<sub>2</sub>W(CCH)(SiH<sub>2</sub>) (**6**) (see ref 7 for the optimized geometry of **6**). The W–vinyl bond of **5** is considerably weaker than the W–acetylido bond of **6** by 31.5 (35.1) kcal/mol (see Supporting Information Table S5), which is consistent with the large difference between the W–vinyl and W–acetylido bond energies in **2** and **4**. This reason is interpreted in terms of the energy difference in the valence orbitals between the vinyl and acetylido groups; the sp lone pair orbital of the acetylido is at lower energy (−11.1 eV) than the sp<sup>2</sup> lone pair orbital (−6.6 eV) of the vinyl group, where the Kohn–Sham orbital energies are presented.<sup>28</sup> Because these orbitals are at lower energy than the SOMO of \*Cp(CO)<sub>2</sub>W(SiH<sub>2</sub>), which is at −5.2 eV,<sup>28</sup> the energy difference between the valence orbitals of the Cp(CO)<sub>2</sub>W(SiH<sub>2</sub>) and acetylido groups is larger than that between the Cp(CO)<sub>2</sub>W(SiH<sub>2</sub>) and vinyl groups, which leads to the stronger W–acetylido bond than the W–vinyl bond; see eq 1.

We also evaluated the W–silylene bond energy in **5** and **6**. The pure W–silylene bond energies are similar in both **5** and **6** (see Supporting Information Table S6), as expected. On the other hand, the W–silylene bond of **2** is stronger than that of **4**, as discussed above. This is because the sp<sup>2</sup> lone pair orbital of the silylene expands toward the W center in **2** but it considerably deviates from the W–Si line in **4**; it makes angles

(28) The geometries of \*CHCH<sub>2</sub>, \*CCH, and \*Cp(CO)<sub>2</sub>W(SiH<sub>2</sub>) were taken to be the same as those in **5** and **6**.

Scheme 6



of  $7.5^\circ$  and  $35.4^\circ$  with the W–Si bond in **2** and **4**, respectively. This significantly large difference arises from the difference between the silylene–vinyl and silylene–acetylidyne interactions, which will be discussed below.

**Reasons Why the Interaction between the Silylene and Vinyl Groups Is Weaker Than That between the Silylene and Acetylidyne Groups.** It is also very important to clarify the reason why the silylene–vinyl interaction is much weaker than the silylene–acetylidyne interaction. A strong CT between the silylene and acetylidyne moieties is observed in **4**, as discussed previously.<sup>7</sup> Unlike **4**, on the other hand, a weak CT is observed between the silylene and vinyl moieties in **2**, as discussed above. First, we examined the  $\pi$  and  $\pi^*$  orbitals of the vinyl and acetylidyne groups. The  $\pi$  and  $\pi^*$  orbitals are at  $-7.6$  and  $-0.4$  eV, respectively, in the vinyl group and at  $-9.1$  and  $-1.3$  eV, respectively, in the acetylidyne group.<sup>29</sup> These results suggest that the  $\pi$  orbital of vinyl forms a stronger CT with the empty p orbital of silylene but the  $\pi^*$  orbital of vinyl forms a weaker CT with the  $\text{sp}^2$  lone pair orbital of silylene. Usually, silylene is considered to be electron-accepting. Thus, the former CT is more important than the latter one, which leads to the expectation that the silylene–vinyl interaction is stronger than the silylene–acetylidyne interaction. This is not consistent with the computational results. Thus, the  $\pi$  and  $\pi^*$  orbital energies of the vinyl group are not responsible for the weak interaction between the silylene and vinyl groups, and another factor must be responsible for it.

The  $\pi$  orbital of the vinyl group is perpendicular to the  $\text{C}=\text{C}$  bond and does not expand well toward the empty p orbital of the silylene moiety, as shown in Scheme 6A. This is because the  $\text{sp}^2$  orbital of the vinyl group must expand toward the W center and, therefore, the  $\text{C}=\text{C}$  double bond deviates from the best position to form the CT interaction with the silylene group; in other words, its  $\pi$  orbital cannot overlap well with the empty p orbital of the silylene group, and the CT interaction between the silylene and vinyl groups is weak in **2**. On the other hand, the sp orbital of the acetylidyne group is collinear with the  $\text{C}\equiv\text{C}$  bond, and the  $\pi$  and  $\pi^*$  orbitals of acetylidyne are cylindrical around the  $\text{C}\equiv\text{C}$  triple bond, as shown in Scheme 6B. Thus, the  $\text{C}\equiv\text{C}$  triple bond can form a strong CT with the silylene moiety in **4**.

## Conclusions

The geometry and bonding nature of interesting new tungsten  $\eta^3$ -silaallyl/ $\eta^3$ -vinylsilyl complex **1** and tungsten vinyl silylene

complex **2** and the conversion reaction of **1** to **2** were theoretically investigated with the DFT, MP2 to MP4(SDTQ), and CCSD(T) methods, where **1** was adopted as a model of  $\text{Cp}^*(\text{CO})_2\text{W}(\eta^3\text{-Me}_2\text{SiCHCMe}_2)$ . The nonbonding  $\pi$  orbital ( $\varphi_{\text{nz}}$ ) of the  $\eta^3\text{-H}_2\text{SiCHCH}_2$  moiety of **1** is similar to that of the  $\eta^3$ -allyl group except that the Si p orbital contributes more to  $\varphi_{\text{nz}}$  than the C p orbital. On the other hand, the  $\pi$  orbital ( $\varphi_{\pi}$ ) of **1** is considerably different from that of the  $\eta^3$ -allyl group; the  $\pi$ -conjugation between the Si and C atoms is very weak, unlike that of the  $\eta^3$ -allyl group in which  $\pi$ -conjugation is considerably strong. Thus, **1** can be understood to be a species between tungsten  $\eta^3$ -vinylsilyl and tungsten  $\eta^3$ -silaallyl complexes.

Because our previous work indicated that similar tungsten  $\eta^3$ -silapropargyl/ $\eta^3$ -alkynylsilyl complex **3** easily converted to tungsten acetylidyne silylene complex **4**, we theoretically investigated tungsten vinyl silylene complex **2**, which is similar to **4**. The  $\text{sp}^2$  lone pair orbital of the silylene group expands toward the W center in **2**, and therefore, a strong W–silylene interaction is formed in **2**, while a very weak CT interaction is formed between the vinyl and silylene groups in **2**. From these results, **2** is understood to be a pure tungsten vinyl silylene complex, unlike **4** in which a strong CT interaction is formed between the acetylidyne and silylene groups.

Complex **1** is much more stable than **2** by 21.0 (20.9) kcal/mol, while **3** is less stable than **4** by 0.7 (4.9) kcal/mol. These differences can be interpreted as follows: Though the Si–C bond is weak in **1**, the W–( $\eta^3\text{-H}_2\text{SiCHCH}_2$ ) interaction is considerably strong. Moreover, the W–vinyl and silylene–vinyl interactions are very weak in **2**. As a result, **1** is much more stable than **2**. On the other hand, the Si–C bond is strong in **3**, but the W–( $\eta^3\text{-H}_2\text{SiCCH}$ ) interaction is weak. Moreover, the W–acetylidyne and silylene–acetylidyne interactions are very strong in **4**. As a result, **3** is less stable than **4**. Thus, **1** can be isolated but **2** cannot, while **4** can be isolated but **3** cannot.

Complex **1** converts to **2** with a large activation barrier of 34.2 (33.2) kcal/mol, while **3** easily converts to **4** with a moderate activation barrier of 15.8 (15.3) kcal/mol. The larger activation barrier of the conversion reaction of **1** to **2** can be interpreted as follows: The coordinate bond of the  $\text{C}=\text{C}$  double bond with the W center is much stronger in **1** than in **3**. This coordinate bond of the  $\text{C}=\text{C}$  double bond is almost broken in the transition state. Thus, this bond breaking induces a large energy loss, which is one of the origins of the large activation barrier.

It is worth discussing the significantly large differences between **1** and **3** and between **2** and **4**. The  $\varphi_{\pi}$  orbital of  $\text{H}_2\text{SiCHCH}_2$  is at higher energy than that of  $\text{H}_2\text{SiCCH}$ , which leads to formation of a stronger W–( $\eta^3\text{-H}_2\text{SiCHCH}_2$ ) interaction of **1** than the similar W–( $\eta^3\text{-H}_2\text{SiCCH}$ ) interaction of **3**. The energy difference between the  $\text{sp}^2$  orbital of vinyl and the SOMO of  $\text{Cp}(\text{CO})_2\text{W}(\text{SiH}_2)$  is much smaller than that between the sp orbital of acetylidyne and the SOMO of  $\text{Cp}(\text{CO})_2\text{W}(\text{SiH}_2)$ , and therefore, the W–vinyl bond of **2** is considerably weaker than the W–acetylidyne bond of **4** because the covalent bond energy increases with an increase in the energy difference between two orbitals. The vinyl group interacts with the W center using its  $\text{sp}^2$  orbital, which leads to a very unfavorable orientation of the  $\text{C}=\text{C}$  double bond for the interaction with silylene. On the other hand, the acetylidyne group interacts with the W center using its sp orbital and the  $\pi$  and  $\pi^*$  orbitals surround the  $\text{C}\equiv\text{C}$  triple bond in a cylindrical way, characteristics of which are favorable for the interaction with silylene. As a result, the silylene–vinyl interaction in **2** is much weaker than the silylene–acetylidyne

(29) The geometries of the vinyl and acetylidyne groups were taken to be the same as those in **2** and **4**, respectively.

interaction of **4**. These results indicate that the tungsten  $\eta^3$ -silaallyl/ $\eta^3$ -vinylsilyl complex **1** can be isolated but the tungsten vinyl silylene complex **2** cannot, unlike the tungsten acetylidc silylene complex  $\text{Cp}(\text{CO})_2\text{W}(\text{CCH})(\text{SiH}_2)$  **4**.

From these results, we emphasize that the isolation of  $\text{Cp}(\text{CO})_2\text{W}(\eta^3\text{-R}^1\text{SiCCR}^2)$  is challenging and also predict that a variety of transition-metal  $\eta^3$ -silaallyl/ $\eta^3$ -vinylsilyl complexes can be synthesized by a method similar to that of the Sakaba and Tilley groups.

**Acknowledgment.** This work was financially supported by Grants-in-Aid on Basic Research (No. 1835005), Priority Areas for "Molecular Theory" (No. 420), Creative Scientific Research, and the NAREGI project from the Ministry of Education,

Science, Sports, and Culture. Some theoretical calculations were performed with SGI workstations of the Institute for Molecular Science (Okazaki, Japan).

**Supporting Information Available:** Complete reference for Gaussian 03, several important Kohn-Sham orbitals observed in **3**, geometries of  $\text{H}_3\text{SiCCH}$ ,  $\text{H}_3\text{SiCHCH}_2$ ,  $^*\text{CHCH}_2$ , and  $^*\text{CCH}$ , W–vinyl and W–acetylidc interaction energies in **5** and **6**, respectively, W–silylene interaction energies in **5** and **6**, total electron populations of **1–4**, and Cartesian coordinates and total energies of important species including transition states. This material is available free of charge via the Internet at <http://pubs.acs.org>.

OM7005563